Journal of Electromagnetic Waves and Applications, Vol. 4, No. 9, 865-891, 1990

Scattering from Variable Resistive and Impedance Sheets

K. Sarabandi

Radiation Laboratory
Department of Electrical Engineering
and Computer Science
University of Michigan
Ann Arbor, MI 48109-2122, USA

Abstract– Scattering from variable planar resistive and impedance sheets with one dimensional variations is studied in this report. An approximate solution is obtained using a perturbation technique in the Fourier domain. It is shown that the solution for a variable resistive sheet with resistivity $R(x)$ is identical to the solution for an impedance surface with impedance $\eta(x)$ by replacing $R(x)$ with $\eta(x)/2$. The solution for the induced current on the sheet in terms of the resistivity (impedance) function is given in a recursive form. The closed form nature of the solution enables us to study the statistical behavior of the scattered field when the perturbation function is a random process. The solutions based on the perturbation technique are compared with those obtained by other methods such as the moment method for periodic resistive and impedance sheets (Appendix A), numerical solution of the integral equation for scattering from a dielectric object above a resistive sheet, and GTD for the problem of impedance insert.

1. INTRODUCTION

In view of the difficulties associated with obtaining exact solutions of Maxwell's equations under given initial and boundary conditions, approximate solutions are often sought instead. A common approximation technique is perturbation theory which is useful primarily when the problem under consideration closely resembles one whose exact solution is known. Perturbational methods have been successfully used for many problems such as cavity and waveguide problems [11,2], scattering from stratified media [1], and scattering from rough metallic surfaces [6]. The resistive sheet and impedance surface approximations have extensively been used in scattering problems [8,10,5] where the resistivity and the impedance are constant.

In this paper we will employ a perturbation method to solve the scattering problem of variable resistive and impedance sheets. Study of this problem is motivated by number of important applications. For example, a thin dielectric slab whose thickness and dielectric constant are non-uniform provides a model for a vegetation leaf, and can be approximated by a resistive sheet with variable resistivity. The variable resistivity $R(x)$ is an explicit function of the thickness and material properties of the slab. Another variable resistive sheet of concern is a periodic resistive sheet, with application to spatial filters and polarizers. Characterization of the scattering behavior of a variable impedance surface is also a matter of increasing concern since dielectric coated perfect conductors can be

modeled by a surface impedance, and a variation of the material property of a terrain surface can be represented by a variable impedance surface.

The approximate solution is obtained using a perturbation technique in the Fourier domain. The solution for the induced current on the sheet in terms of the resistivity function is given in a recursive form. The closed form nature of the solution enables us to study the statistical behavior of the scattered field when the resistivity function is a random process. The solution for the current on an impedance surface with impedance $\eta(x)$ is identical with that of the resistive sheet and can be obtained by replacing $R(x)$ with $\eta(x)/2$.

The solution to any desired order for a periodic perturbation is obtained analytically and the results are compared with an exact solution obtained using a moment method which is developed in Appendix A. The technique is also used to characterize the scattering behavior of a thin dielectric slab with a hump and the solution is compared to that obtained using the moment method in conjunction with the exact image theory for resistive sheets [7]. To demonstrate the ability of this perturbation technique to handle sharp variations in the spatial domain, the problem of scattering from an impedance insert is considered and compared with a uniform GTD solution [4].

2. DERIVATION OF INTEGRAL EQUATION FOR RESISTIVE AND IMPEDANCE SHEETS

The resistive sheet is simply an electric current sheet modelling a thin dielectric layer capable of supporting electric current. The electric current on the sheet is proportional to the tangential electric field and the proportionality constant is denoted by a complex resistivity R given by

$$R = \frac{iZ_0}{k_0\tau(\epsilon - 1)} \tag{1}$$

Here, $Z_0 (= 1/Y_0)$ and k_0 are the characteristic impedance and propagation constant, respectively, of free space. Also τ and $\epsilon = \epsilon' + i\epsilon''$ are the thickness and the dielectric constant of the dielectric layer, respectively, and for convenience a time factor $e^{-i\omega t}$ has been assumed and suppressed.

The electromagnetic boundary conditions that govern the fields on the resistive sheet are given by [9]

$$[\hat{n} \times \overline{E}]_-^+ = 0 \tag{2}$$

$$\hat{n} \times (\hat{n} \times \overline{E}) = -R\overline{J} \tag{3}$$

$$\overline{J} = [\hat{n} \times \overline{H}]_-^+ \tag{4}$$

where $\hat{n}$ is the unit vector normal to the top $(+)$ side of the sheet, $\overline{J}$ is the induced current on the sheet, and $[\ ]_-^+$ denotes the discontinuity across the sheet.

Consider a planar resistive sheet occupying the xy-plane and having a resistivity which is only a function of x. Suppose a plane wave is incident on the sheet at an angle ϕ_0 measured from the normal. The geometry of the problem is depicted

in Fig. 1. For the E-polarization case where the electric field is perpendicular to the plane of incidence, we assume

$$\overline{E}^i = \hat{y} e^{ik_0(\sin\phi_0 x - \cos\phi_0 z)} \tag{5}$$

The induced current in this case has only a y-component and the scattered field due to this current is found to be

$$\overline{E}^s(\vec{\rho}) = -\hat{y}\frac{k_0 Z_0}{4}\int_{-\infty}^{+\infty} J_y(x') H_0^{(1)}\left(k_0|\overline{\rho} - \overline{\rho}'|\right) dx' \tag{6}$$

where $H_0^{(1)}$ is the Hankel function of first kind and zeroth-order. The induced current and the total electric field given by

$$\overline{E}^t = \overline{E}^i + \overline{E}^s \tag{7}$$

must satisfy the boundary condition given by (3). Noting that $\hat{n} = \hat{z}$ and substituting for $\overline{E}^i$ and $\overline{E}^s$ from (5) and (6), the following integral equation for the induced current can be obtained:

$$R(x)J_y(x) = e^{ik_0 \sin\phi_0 x} - \frac{k_0 Z_0}{4}\int_{-\infty}^{+\infty} J_y(x') H_0^{(1)}\left(k_0|x - x'|\right) dx' \tag{8}$$

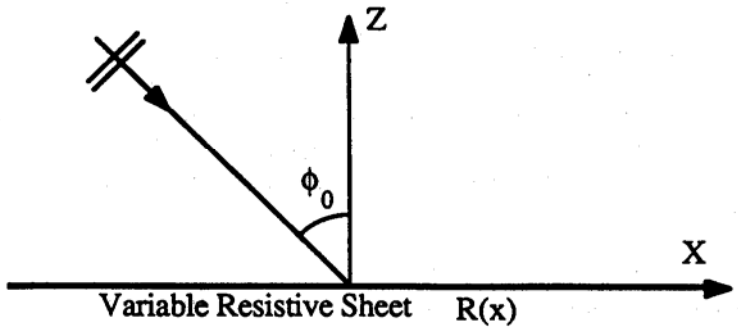

Figure 1. Geometry of the scattering problem for a variable resistive sheet.

For the H-polarization case in which the magnetic field vector is perpendicular to the plane of incidence, we have

$$\overline{E}^i = -(\cos\phi_0\,\hat{x} + \sin\phi_0\,\hat{z})\, e^{ik_0(\sin\phi_0 x - \cos\phi_0 z)} \tag{9}$$

In this case the induced current has only an x-component and

$$E_x^s(x,z) = -\frac{k_0 Z_0}{4}\int_{-\infty}^{+\infty} J_x(x')\left(1 + \frac{1}{k_0^2}\frac{\partial^2}{\partial x^2}\right) H_0^{(1)}\left(k_0\sqrt{(x-x')^2 + z^2}\right) dx' \tag{10}$$

By obtaining the total field at the surface of the sheet and applying the boundary condition (3) the following integral equation for the induced current in the H-polarization case can be derived:

$$R(x)J_x(x) = -\cos\phi_0\, e^{ik_0 \sin\phi_0 x} - \frac{k_0 Z_0}{4}\int_{-\infty}^{+\infty} J_x(x')\left(1+\frac{1}{k_0^2}\frac{\partial^2}{\partial x^2}\right) H_0^{(1)}\left(k_0|x-x'|\right)\, dx' \quad (11)$$

Now consider an impedance surface occupying the xy-plane. Suppose the impedance is a function only of the variable x and is denoted by $\eta(x)$ (see Fig. 1). The boundary condition on the surface is

$$\hat{n}\times(\hat{n}\times\overline{E}) = -\eta(x)\,\hat{n}\times\overline{H} \quad (12)$$

The field scattered from this surface can be obtained by replacing the total tangential magnetic field on the surface by an electric current over a perfect magnetic conductor using the field equivalence principle [3]. The equivalent electric current is

$$\overline{J} = \hat{n}\times\overline{H} \quad (13)$$

and by invoking image theory, the magnetic wall can be removed by doubling the electric current.

In the E-polarization case the total tangential magnetic field on the surface is in the x-direction which implies that the electric current is in the y-direction. The scattered electric field can be obtained from expression (6) by doubling the electric current. The total electric field on the surface is composed of the incident field, the field reflected from the magnetic wall, and the scattered field. From (12) and (13) we have

$$\left[E_y^i + E_y^r + E_y^s\right]_{z=0} = \eta(x)\, J_y(x) \quad (14)$$

which leads to the following integral equation for the electric current:

$$\frac{\eta(x)}{2}\, J_y(x) = e^{ik_0\sin\phi_0 x} - \frac{k_0 Z_0}{4}\int_{-\infty}^{+\infty} J_y(x')H_0^{(1)}\left(k_0|x-x'|\right)\, dx' \quad (15)$$

When the incident field is H-polarized the total tangential magnetic field is in the y-direction which implies that the equivalent electric current flows in the x-direction. The tangential scattered electric field can be obtained from (10) by doubling the electric current. Also, from the boundary condition (12), we have

$$\left[E_x^i + E_x^r + E_x^s\right]_{z=0} = \eta(x)\, J_x(x) \quad (16)$$

Upon substituting the appropriate quantities from (9) and (10) into the above equation we get:

$$\frac{\eta(x)}{2}\, J_x(x) = -\cos\phi_0\, e^{ik_0\sin\phi_0 x} - \frac{k_0 Z_0}{4}\int_{-\infty}^{+\infty} J_x(x')\left(1+\frac{1}{k_0^2}\frac{\partial^2}{\partial x^2}\right) H_0^{(1)}\left(k_0|x-x'|\right)\, dx' \quad (17)$$

Note that the integral equations obtained for the impedance sheet are identical to those obtained for the resistive sheet if $R(x)$ is replaced by $\eta(x)/2$. Therefore all the analysis that will be carried out for the resistive sheet can be applied to the corresponding impedance sheet.

3. PERTURBATION SOLUTION

The integral equations for the induced current on the resistive sheet are Fredholm integral equations of the second type, and for an arbitrary resistivity function $R(x)$ there is no known technique for finding their exact solution. Here we obtain an approximate iterative solution to these integral equations using a perturbation technique and Fourier transform. For the sake of simplicity let us represent the integral equations (8) and (11) by the following equation:

$$R(x)\,J(x) = a\,e^{ik_0 \sin\phi_0 x} - \frac{k_0 Z_0}{4}\,(J * g)(x) \tag{18}$$

where $g(x)$ is the kernel of the integral equation, a is 1 or $-\cos\phi_0$ for E- or H-polarization respectively, and $(J * g)(x)$ denotes the convolution integral. By taking the Fourier transform of (18), the integral equation in the Fourier domain becomes

$$\frac{1}{2\pi}\left(\tilde{R} * \tilde{J}\right)(\alpha) = 2\pi a\,\delta(\alpha - k_0 \sin\phi_0) - \frac{k_0 Z_0}{4}\,\tilde{J}(\alpha)\tilde{g}(\alpha) \tag{19}$$

where the Fourier transform of functions are denoted by a $\tilde{}$ and δ is the Dirac delta function. The transform of the kernel function is given by

$$\tilde{g}(\alpha) = \begin{cases} \dfrac{2}{\sqrt{k_0^2 - \alpha^2}}, & E\text{-polarization} \\ \dfrac{2}{k_0^2}\sqrt{k_0^2 - \alpha^2}, & H\text{-polarization} \end{cases} \tag{20}$$

where the branch of square root is defined such that $\sqrt{-1} = i$. When the resistivity of the sheet is constant, an exact solution to the integral equation (18) can be obtained, and if $R(x) = R_0$, then

$$\tilde{R}(\alpha) = 2\pi R_0\,\delta(\alpha) \tag{21}$$

The transform of the current can be obtained from (19) and is given by

$$\tilde{J}_0(\alpha) = \frac{a\,[2\pi\delta(\alpha - k_0 \sin\phi_0)]}{R_0 + \dfrac{k_0 Z_0}{4}\,\tilde{g}(\alpha)} \tag{22}$$

and the current in the spatial domain for E- and H-polarization respectively are

$$\overline{J}_0^e(x) = \hat{y}\,\frac{2Y_0 \cos\phi_0}{1 + 2R_0 Y_0 \cos\phi_0}\,e^{ik_0 \sin\phi_0 x} \tag{23}$$

$$\overline{J}_0^h(x) = \hat{x}\,\frac{-2Y_0 \cos\phi_0}{2R_0 Y_0 + \cos\phi_0}\,e^{ik_0 \sin\phi_0 x} \tag{24}$$

which are identical to the result obtained from a plane wave reflection coefficient calculation [9].

If the resistivity has a small variation as a function of position, let

$$R(x) = R_0\,(1 + \Delta r(x)) \tag{25}$$

where $r(x)$ is the perturbation function assuming $|r(x)| \leq 1$ and Δ is a complex constant ($|\Delta| < 1$). The induced current on the sheet is assumed to be

$$J(x) = \sum_{n=0}^{+\infty} J_n(x)\Delta^n \tag{26}$$

where $J_n(x)$ denotes the nth component of the induced current. Obviously, if $\Delta = 0$ then $J(x) = J_0(x)$. From (25) and (26)

$$\widetilde{R}(\alpha) = 2\pi R_0\,\delta(\alpha) + R_0\,\widetilde{r}(\alpha)\Delta \tag{27}$$

$$\widetilde{J}(\alpha) = \sum_{n=0}^{+\infty} \widetilde{J}_n(\alpha)\Delta^n \tag{28}$$

and when substituted into (19), the terms given by (22) can be cancelled, and the remaining terms can be written as

$$\sum_{n=1}^{+\infty} \left\{ R_0 \left[\widetilde{J}_n(\alpha) + \frac{1}{2\pi}\,\widetilde{r}(\alpha) * \widetilde{J}_{n-1}(\alpha) \right] + \frac{k_0 Z_0}{4}\,\widetilde{g}(\alpha)\,\widetilde{J}_n(\alpha) \right\} \Delta^n = 0 \tag{29}$$

Since this must hold for any value of Δ, all of the coefficients must be zero. Thus for E-polarization

$$\widetilde{J}_n^e(\alpha) = -2Y_0R_0 \cdot \frac{\sqrt{1 - \frac{\alpha^2}{k_0^2}}}{1 + 2Y_0R_0\sqrt{1 - \frac{\alpha^2}{k_0^2}}} \cdot \frac{1}{2\pi} \left(\widetilde{r} * \widetilde{J}_{n-1}^e \right)(\alpha) \tag{30}$$

and for H-polarization we have

$$\widetilde{J}_n^h(\alpha) = -2Y_0R_0 \cdot \frac{1}{2Y_0R_0 + \sqrt{1 - \frac{\alpha^2}{k_0^2}}} \cdot \frac{1}{2\pi} \left(\widetilde{r} * \widetilde{J}_{n-1}^h \right)(\alpha) \tag{31}$$

The above recursive relations along with the expressions for $\widetilde{J}_0(\alpha)$ can be used to derive the induced currents to any desired order of approximation. The first-order solution can be obtained very easily and the transforms of the first component of the induced current for E and H-polarizations are

$$\widetilde{J}_1^e(\alpha) = \frac{-4Y_0^2R_0\cos\phi_0}{1 + 2Y_0R_0\cos\phi_0} \cdot \frac{\sqrt{1 - \frac{\alpha^2}{k_0^2}}}{1 + 2Y_0R_0\sqrt{1 - \frac{\alpha^2}{k_0^2}}}\,\widetilde{r}(\alpha - k_0\sin\phi_0) \tag{32}$$

$$\widetilde{J}_1^h(\alpha) = \frac{4Y_0^2R_0\cos\phi_0}{\cos\phi_0 + 2Y_0R_0} \cdot \frac{1}{2Y_0R_0 + \sqrt{1 - \frac{\alpha^2}{k_0^2}}}\,\widetilde{r}(\alpha - k_0\sin\phi_0) \tag{33}$$

The complexity of obtaining high-order solutions depends on the perturbation function $r(x)$.

4. PERIODIC RESISTIVITY

A simple case where it is possible to determine the nth components of the induced currents is a periodic resistivity with period L. In this case we can write

$$r(x) = \sum_{m=-\infty}^{+\infty} c_m e^{i\frac{2\pi m}{L}x} \tag{34}$$

and the Fourier transform of the perturbation function is

$$\tilde{r}(\alpha) = 2\pi \sum_{m=-\infty}^{+\infty} c_m \delta\left(\alpha - \frac{2\pi m}{L}\right) \tag{35}$$

For the E-polarization case the transform of the nth component of the induced current can be obtained from (30) and (35) and is

$$\tilde{J}_n^e(\alpha) = -2Y_0R_0 \cdot \frac{1}{2Y_0R_0 + \sqrt{1 - \frac{\alpha^2}{k_0^2}}} \cdot \sum_{m=-\infty}^{+\infty} c_m \tilde{J}_{n-1}^e\left(\alpha - \frac{2\pi m}{L}\right) \tag{36}$$

By employing the expression (22) for $\tilde{J}_0(\alpha)$ and after some algebraic manipulation, a closed form for the nth components of the induced current in the spatial domain can be obtained:

$$\begin{aligned} J_n^e(x) = {} & \frac{-2Y_0R_0\cos\phi_0(-2Y_0R_0)^n}{1 + 2Y_0R_0\cos\phi_0} \\ & \cdot \sum_{m_n=-\infty}^{+\infty} \cdots \sum_{m_1=-\infty}^{+\infty} \left[\prod_{i=1}^{n} \frac{\sqrt{1 - \left(\sin\phi_0 + \frac{\lambda}{L}\sum_{j=1}^{i} m_j\right)^2}}{1 + 2Y_0R_0\sqrt{1 - \left(\sin\phi_0 + \frac{\lambda}{L}\sum_{j=1}^{i} m_j\right)^2}}\right] \\ & \cdot c_{m_n} \cdots c_{m_1} e^{i\left(k_0\sin\phi_0 + \frac{2\pi}{L}\sum_{\ell=1}^{n} m_\ell\right)x} \end{aligned} \tag{37}$$

A problem associated with the perturbation techniques is that when there is a sharp variation in the perturbation function there could be a sharp variation in the solution which is not to the order of perturbation. Therefore in an nth order solution it is not guaranteed that the solution is of $O(\Delta^{n+1})$ for all values of the variable in the domain of the integral equation. To check the validity of our assumption we consider two limiting cases: (1) when the perturbation function has sharp variations in the spatial domain and (2) when the perturbation function has sharp variations in the Fourier domain. The first case will be studied in Section 6 and to study the latter case we consider a constant function $(r(x) = 1)$ for the perturbation function. Note that the perturbation technique was applied to the integral equation (19), and in this case the perturbation function $\tilde{r}(\alpha) = 2\pi\delta(\alpha)$ has the sharpest variation possible. When $r(x) = 1$ the resistivity is constant and from equation (23) it follows directly that

$$J_0^e(x) = \frac{2Y_0\cos\phi_0}{1 + 2Y_0R_0(1+\Delta)\cos\phi_0} e^{ik_0\sin\phi_0 x} \tag{38}$$

The solution based on the perturbation technique can be obtained from equation (37) with $L = \infty$, $c_0 = 1$ and $c_m = 0$ (for $m \neq 0$); thus

$$J^e(x) = \sum_{n=0}^{+\infty} \frac{2Y_0 \cos\phi_0 (-2Y_0R_0)^n}{(1+2Y_0R_0\cos\phi_0)^{n+1}} e^{ik_0 \sin\phi_0 x} \Delta^n \tag{39}$$

This series is absolutely convergent and represents the Taylor series expansion of (38), implying that the perturbation solution can be made as close as we wish to the exact solution.

For H-polarization the analysis is similar and the expression for the component of the induced current in the spatial domain is:

$$J_n^h(x) = \frac{-2Y_0R_0\cos\phi_0 (-2Y_0R_0)^n}{2Y_0R_0 + \cos\phi_0} \cdot \sum_{m_n=-\infty}^{+\infty} \cdots \sum_{m_1=-\infty}^{+\infty} \prod_{i=1}^{n} \frac{1}{2Y_0R_0 + \sqrt{1 - \left(\sin\phi_0 + \frac{\lambda}{L}\sum_{j=1}^{i} m_j\right)^2}} \cdot c_{m_n} \cdots c_{m_1} e^{i\left(k_0 \sin\phi_0 + \frac{2\pi}{L}\sum_{\ell=1}^{n} m_\ell\right)x} \tag{40}$$

In Appendix A a numerical solution for a periodic resistive sheet is given. The solution is based on the moment method, and in Section 7 the results are compared with the above perturbation solution.

The closed form expression for the induced current enables us to study the case when the perturbation is a periodic random process. In this case the perturbation function may still be represented as a Fourier series but with the Fourier coefficients ($c_m's$) as random variables. It can be shown from ($A13$) that the average value of the diffracted field is directly proportional to the average value of the induced current.

5. SCATTERING MODEL FOR A VARIABLE THICKNESS DIELECTRIC SLAB

Consider a dielectric slab whose thickness is a function of x (see Fig. 2). Let the thickness be

$$T(x) = \tau_0 \left(1 + \frac{w^2}{x^2 + w^2} \cdot \Delta\right) \tag{41}$$

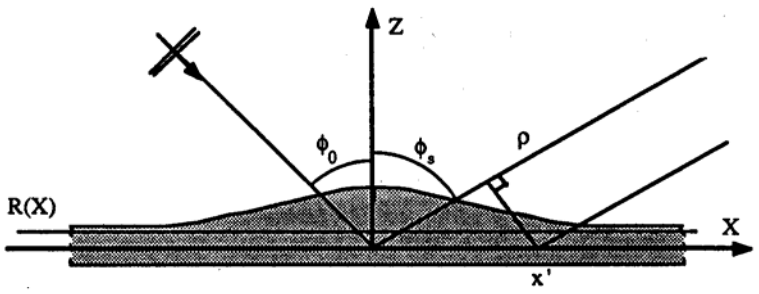

Figure 2. Geometry of a dielectric slab with a hump.

where w is a measure of the width and Δ is the height of the dielectric hump. This thickness function resembles the variation in thickness of a vegetation leaf and in this case w and Δ are random variables. If the dielectric slab is electrically thin and $\Delta \ll 1$, the resistivity function can be obtained from (1) and to the first order of Δ it can be shown

$$R(x) \simeq R_0 \left(1 - \frac{w^2}{x^2 + w^2}\Delta\right) \tag{42}$$

where R_0 is the resistivity of the slab corresponding to $\Delta = 0$. The perturbation function then takes the form

$$r(x) = \frac{-w^2}{x^2 + w^2} \tag{43}$$

The Fourier transforms of the first components of the induced current for E- and H-polarization can be obtained from (32) and (33) respectively, and are

$$\tilde{J}_1^e(\alpha) = \frac{4Y_0^2 R_0 \cos\phi_0}{1 + 2Y_0 R_0 \cos\phi_0} \cdot \frac{\sqrt{1 - \frac{\alpha^2}{k_0^2}}}{1 + 2Y_0 R_0 \sqrt{1 - \frac{\alpha^2}{k_0^2}}} \cdot \left(\pi w\, e^{-w|\alpha - k_0 \sin\phi_0|}\right) \tag{44}$$

$$\tilde{J}_1^h(\alpha) = \frac{-4Y_0^2 R_0 \cos\phi_0}{\cos\phi_0 + 2Y_0 R_0} \cdot \frac{1}{2Y_0 R_0 + \sqrt{1 - \frac{\alpha^2}{k_0^2}}} \cdot \left(\pi w\, e^{-w|\alpha - k_0 \sin\phi_0|}\right) \tag{45}$$

The scattered field due to the zeroth-order induced current consists of reflected and transmitted plane waves in the specular and forward directions, while the first component of the induced current gives rise to a cylindrical wave which will be denoted by the superscript s. In the far zone when ρ and ϕ_s denote the distance and direction of observation point, it is easy to obtain the far field amplitude $\overline{P}(\phi_0, \phi_s)$ defined by

$$\overline{E}^s \simeq \sqrt{\frac{2}{\pi k_0 \rho}}\, e^{i(k_0\rho - \frac{\pi}{4})}\, \overline{P}(\phi_0, \phi_s) \tag{46}$$

in terms of which the bistatic echo width is

$$\sigma(\phi_0, \phi_s) = \frac{2\lambda}{\pi} \left|\overline{P}(\phi_0, \phi_s)\right|^2 \tag{47}$$

In the E-polarization case the scattered field is in the y-direction and

$$\begin{aligned} \overline{P}_e(\phi_0, \phi_s) &= \hat{y}\, \frac{-k_0 Z_0}{4} \int_{-\infty}^{+\infty} J_1^e(x')\, e^{-ik_0 \sin\phi_s x'}\, dx' \\ &= \hat{y}\, \frac{-k_0 Z_0}{4}\, \tilde{J}_1^e(k_0 \sin\phi_s) \end{aligned} \tag{48}$$

For H-polarization, in far zone, the scattered field has only a ϕ-component, and the far field amplitude is

$$\begin{aligned} \overline{P}_h(\phi_0, \phi_s) &= \hat{\phi} \cos\phi_s\, \frac{k_0 Z_0}{4} \int_{-\infty}^{+\infty} J_1^h(x')\, e^{-ik_0 \sin\phi_s x'}\, dx' \\ &= \hat{\phi}\, \frac{k_0 Z_0}{4} \cos\phi_s\, \tilde{J}_1^h(k_0 \sin\phi_s) \end{aligned} \tag{49}$$

Hence, from (44) and (45),

$$\overline{P}_e(\phi_0,\phi_s)=\hat{y}\,\frac{-k_0Y_0R_0\cos\phi_0}{1+2Y_0R_0\cos\phi_0}\cdot\frac{\cos\phi_s}{1+2Y_0R_0\cos\phi_s}\cdot\left(\pi w\Delta e^{-k_0w|\sin\phi_s-\sin\phi_0|}\right) \tag{50}$$

$$\overline{P}_h(\phi_0,\phi_s)=\hat{\phi}\,\frac{-k_0Y_0R_0\cos\phi_0}{\cos\phi_0+2Y_0R_0}\cdot\frac{\cos\phi_s}{2Y_0R_0+\cos\phi_s}\cdot\left(\pi w\Delta e^{-k_0w|\sin\phi_s-\sin\phi_0|}\right) \tag{51}$$

It is now easy to obtain statistical behavior of bistatic scattering width if Δ and/or w are random variables.

The above is a first-order solution, and for a higher order solution, analytical results may not be achievable. When the height of the dielectric hump above the resistive sheet is not much smaller than the wavelength, the above solution fails to work for two reasons: (1) the solution is first-order in Δ, and (2) the dielectric hump cannot be modeled as a single resistive sheet. In such cases we have to resort to numerical techniques to get the solution [7]. Results based on the perturbation technique and a moment method in conjunction with the exact image theory for the resistive sheet are compared in Section 7.

6. SCATTERING FROM IMPEDANCE INSERT

Another application of the perturbation technique is the scattering of a plane wave from the impedance insert whose geometry is shown in Fig. 3. The impedance of this surface can be represented as

$$\eta(x)=\begin{cases}\eta_0(1+\Delta), & |x|\le w/2\\ \eta_0, & \text{otherwise}\end{cases}$$

where w is the width of the insert, and as before, Δ is a constant with $|\Delta|<1$. The transform of the first components of the induced current for E- and H-polarization respectively can be obtained from (32) and (33) by replacing R_0 by $\eta_0/2$ as follows:

$$\tilde{J}_1^e(\alpha)=\frac{-2Y_0^2\eta_0\cos\phi_0}{1+Y_0\eta_0\cos\phi_0}\cdot\frac{\sqrt{1-\frac{\alpha^2}{k_0^2}}}{1+Y_0\eta_0\sqrt{1-\frac{\alpha^2}{k_0^2}}}\,w\frac{\sin\left(w(\alpha-k_0\sin\phi_0)/2\right)}{w(\alpha-k_0\sin\phi_0)/2} \tag{52}$$

$$\tilde{J}_1^h(\alpha)=\frac{2Y_0^2\eta_0\cos\phi_0}{\cos\phi_0+Y_0\eta_0}\cdot\frac{1}{Y_0\eta_0+\sqrt{1-\frac{\alpha^2}{k_0^2}}}\,w\frac{\sin(w(\alpha-k_0\sin\phi_0)/2)}{w(\alpha-k_0\sin\phi_0)/2} \tag{53}$$

Unfortunately, analytical expressions for the higher order components of the induced current cannot be obtained for this case but they can be found numerically. To observe the behavior of the current in the spatial domain, expressions (52) and (53) were transformed numerically and the results are shown in Figs. 4 and 5. They show the expected behavior of the currents at the edges.

The far field amplitudes can be found by doubling the expressions given by (48) and (49). Thus

$$\overline{P}_e(\phi_0,\phi_s) = \hat{y}\frac{-k_0Y_0\eta_0\cos\phi_0}{1+Y_0\eta_0\cos\phi_0}\cdot\frac{\cos\phi_s}{1+Y_0\eta_0\cos\phi_s}\cdot w\Delta\frac{\sin(wk_0(\sin\phi_s-\sin\phi_0)/2)}{wk_0(\sin\phi_s-\sin\phi_0)/2} \tag{54}$$

$$\overline{P}_h(\phi_0,\phi_s) = \hat{\phi}\frac{-k_0Y_0\eta_0\cos\phi_0}{\cos\phi_0+Y_0\eta_0}\cdot\frac{\cos\phi_s}{Y_0\eta_0+\cos\phi_s}\cdot w\Delta\frac{\sin(wk_0(\sin\phi_s-\sin\phi_0)/2)}{wk_0(\sin\phi_s-\sin\phi_0)/2} \tag{55}$$

The results of this technique are compared with a uniform GTD solution [4] that accounts for up to third order diffracted fields in the next Section.

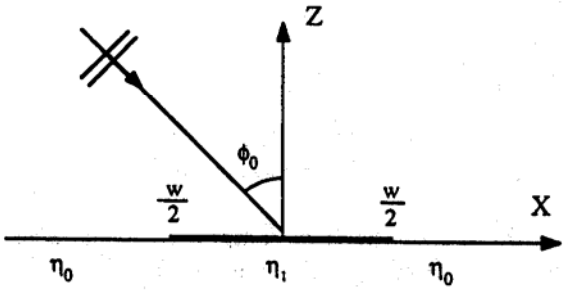

Figure 3. Geometry of an impedance insert.

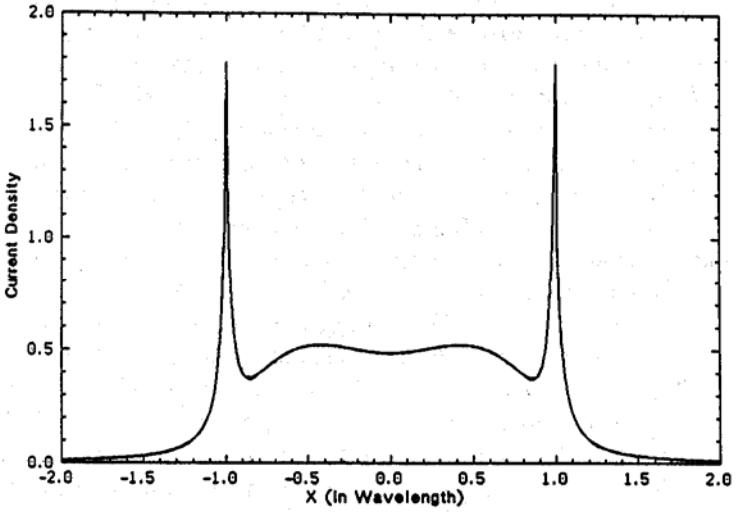

Figure 4. Distribution of the first component of induced current on an impedance insert for E-polarization.

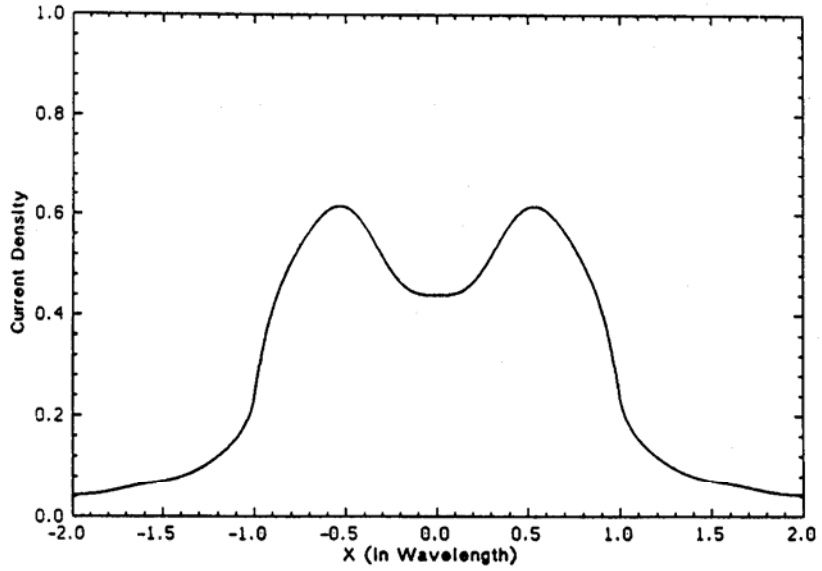

Figure 5. Distribution of the first component of induced current on an impedance insert for H-polarization.

7. NUMERICAL RESULTS

Computations based on the results derived in Sections 3–6 will now be presented and, where possible, compared with data obtained by other methods. First let us consider the periodic resistive sheet. Figures 6 and 7 show the amplitude and phase of the induced current on a resistive sheet with sinusoidal variation of period $L = 2\lambda$ and $\Delta = 0.7$ for E-polarization. In these plots the first through fourth order solutions are presented using the expression (37), and compared with the data obtained by the moment method as given in Appendix A. It is seen that by increasing the order of solution we can get as close as we wish to the exact solution, and that the fourth order solution provides excellent agreement with the moment method data. We note here that the required order is directly proportional to Δ and L/λ. Similar results are shown in Figs. 8 and 9 for H-polarization. The normalized field amplitudes of the propagating modes (Bragg modes) defined in Appendix A are given in Table 1 for a sinusoidal resistivity with $L = 3\lambda$, $\Delta = 0.7$, and $R_0 = 0 + i100$ at angle $\phi_0 = 30$ degrees. Since the resistivity is pure imaginary, there is no power loss and the total power carried by all of the modes is equal to the incident power. Note that apart from the case $n = 0$, $E_n^- = E_n^+$ and $H_n^- = -H_n+$, where $E_n^\pm$ and $H_n^\pm$ are the field amplitudes of nth mode in the upper $(+)$ and lower $(-)$ half-spaces for E and H-polarizations respectively. When $n = 0$ the incident field should be added to the zeroth mode in the lower half-space, i.e., $E_0^- = E_0^+ + E^i$ and $H_0^- = -H_0^+ + H^i$.

We now turn to the problem of a variable thickness dielectric slab. The results of the perturbation technique presented in Section 5 are compared with the numerical solution based on exact image theory for a resistive sheet in conjunction with the moment method. In this numerical solution an integral transformation is used to obtain the Green's function of the problem in a form amenable for numeical calculation [7]. For all of the test cases the dielectric slab is assumed to be homogeneous with $\epsilon = 36 + i17$, $\tau_0 = \lambda/100$, $\Delta = 0.3$, and $\lambda = 3$ cm which correspond to $R_0 = 180 + i270$. Figures 10–13 show the bistatic echo width and the phase of the far field amplitude of a dielectric hump over the resistive sheet for $w = \lambda/15$ and incidence angle $\phi_0 = 0$ for both polarizations. In each figure the results based on the perturbation technique are compared with the numerical results. The agreement is good in spite of the fact that the perturbation solution is only a first order solution.

Figures 14–17 compare the results of the perturbation method and the GTD technique for the impedance insert problem. The figures show the normalized bistatic echo width (σ/λ) of an impedance insert having $w = 2\lambda$ and $\eta_0 = 40 - i40$ using the two methods. The agreement is excellent (for $\Delta = 0.5$ the error is only 0.3 dB) in spite of the sharp changes in the perturbation function in the spatial domain. The spikes in Figs. 14 and 16 are due to the difficulties of evaluating the GTD expressions at the reflection boundary.

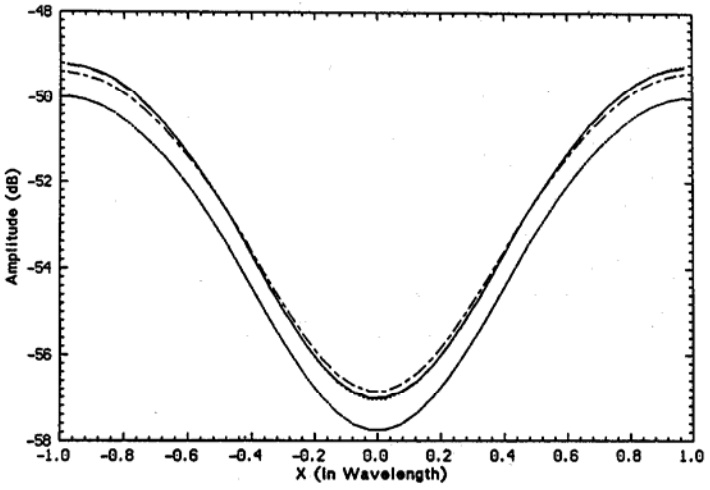

Figure 6. The amplitude of the induced current on a periodic resistive sheet with resistivity $R(x) = (180 + i270)(1 + 0.7\cos 2\pi x/L)$, $L = 2\lambda$ at normal incidence for E-polarization: (——) moment method, (- - - -) fourth order solution, (— —) third order solution, (— - —) second order solution, (— - - - —) first order solution.

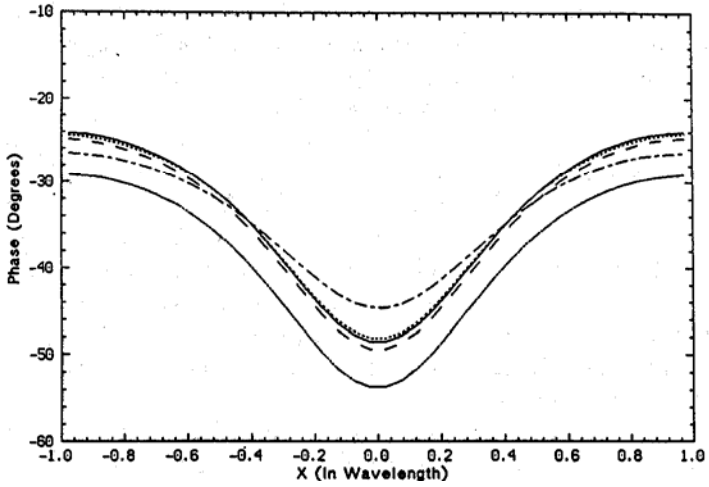

Figure 7. The phase of the induced current on a periodic resistive sheet with resistivity $R(x) = (180 + i270)(1 + 0.7\cos 2\pi x/L)$, $L = 2\lambda$ at normal incidence for E-polarization: (——) moment method, (- - - -) fourth order solution, (— —) third order solution, (— - —) second order solution, (— - - - —) first order solution.

n	E-polarization		H-polarization	
	E_n^+/E^i	E_n^-/E^i	H_n^+/H^i	H_n^-/H^i
-4	0.001∠62.37	0.001∠62.37	0.001∠-150.10	0.001∠29.90
-3	0.003∠169.70	0.003∠169.70	0.004∠-18.57	0.004∠161.43
-2	0.020∠-76.15	0.020∠-76.15	0.022∠99.93	0.022∠-80.07
-1	0.124∠40.43	0.124∠40.43	0.136∠-143.68	0.136∠36.32
0	0.887∠156.86	0.394∠62.13	0.831∠-27.13	0.460∠55.50
1	0.136∠49.53	0.136∠49.53	0.210∠-158.67	0.210∠21.33

Table 1. Normalized field amplitude of the propagating modes in the upper (+) and lower (−) half-spaces for a periodic resistive sheet $R(x) = R_0(1 + 0.7\cos 2\pi x/L)$ with $R_0 = 0 + i100$ and $L = 3\lambda$ at $\phi_0 = 30°$.

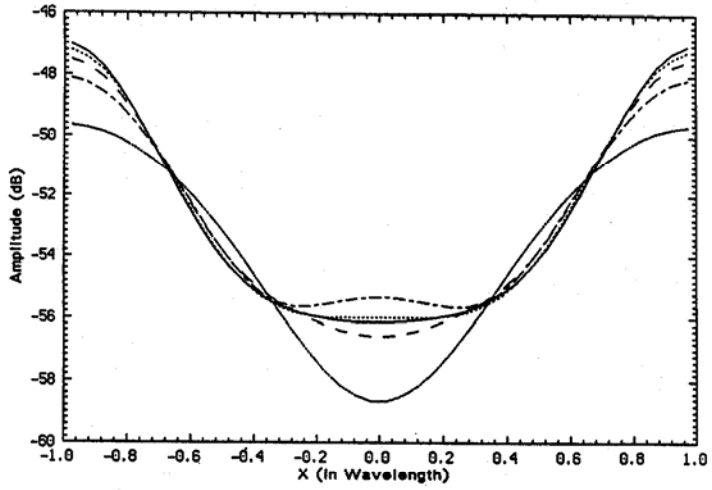

Figure 8. The amplitude of the induced current on a periodic resistive sheet with resistivity $R(x) = (180 + i270)(1 + 0.7\cos 2\pi x/L)$, $L = 2\lambda$ at normal incidence for H-polarization: (——) moment method, (- - - -) fourth order solution, (— —) third order solution, (— – —) second order solution, (— - - - —) first order solution.

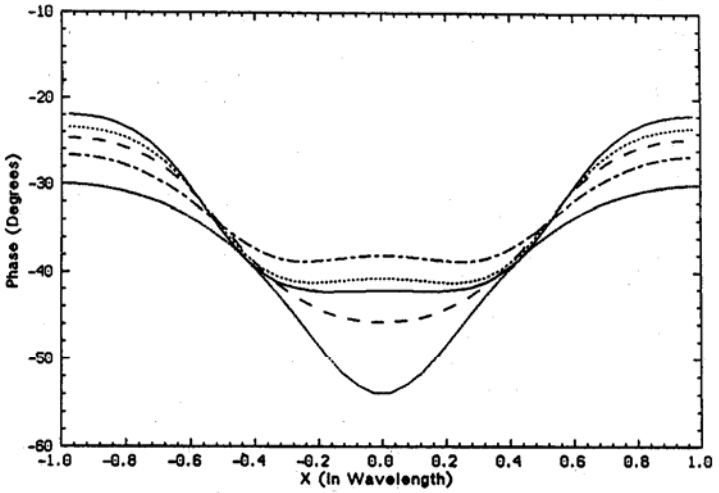

Figure 9. The phase of the induced current on a periodic resistive sheet with resistivity $R(x) = (180 + i270)(1 + 0.7\cos 2\pi x/L)$, $L = 2\lambda$ at normal incidence for H-polarization: (——) moment method, (- - - -) fourth order solution, (— —) third order solution, (— – —) second order solution, (— - - - —) first order solution.

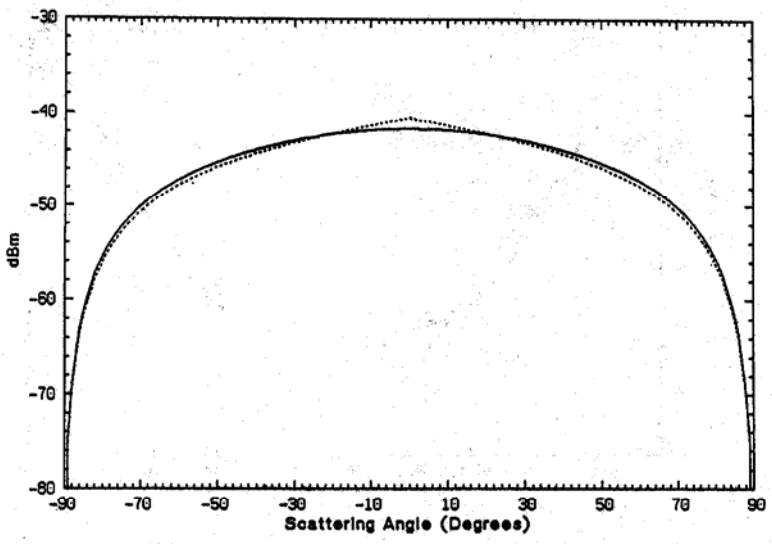

Figure 10. Bistatic echo width of a dielectric hump with $\epsilon = 36+i17$, $\Delta = 0.3$, and $w = \lambda/15$ over a resistive sheet with $R_0 = 180+i270$ at $f = 10\,\text{GHz}$ and $\phi_0 = 0$ degrees for E-polarization: (——) numerical technique, (- - - -) perturbation technique.

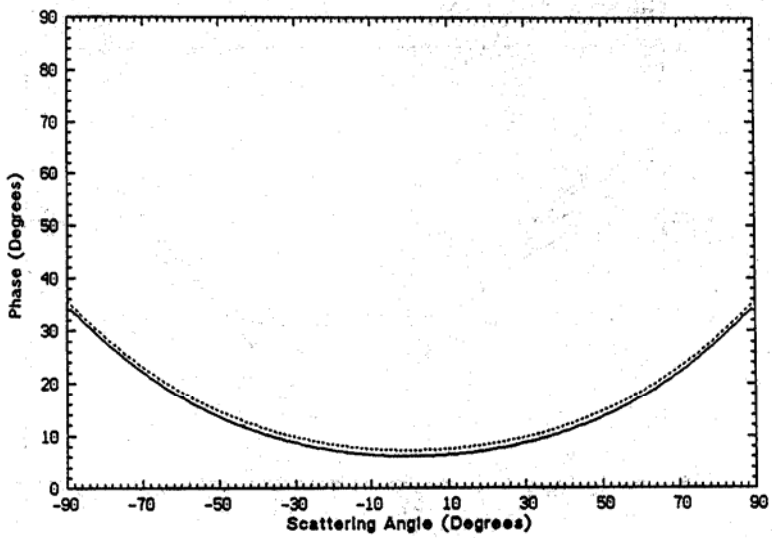

Figure 11. Phase of far field amplitude of a dielectric hump with $\epsilon = 36 + i17$, $\Delta = 0.3$, and $w = \lambda/15$ over a resistive sheet with $R_0 = 180 + i270$ at $f = 10\,\text{GHz}$ and $\phi_0 = 0$ degrees for E-polarization: (——) numerical technique, (- - - -) perturbation technique.

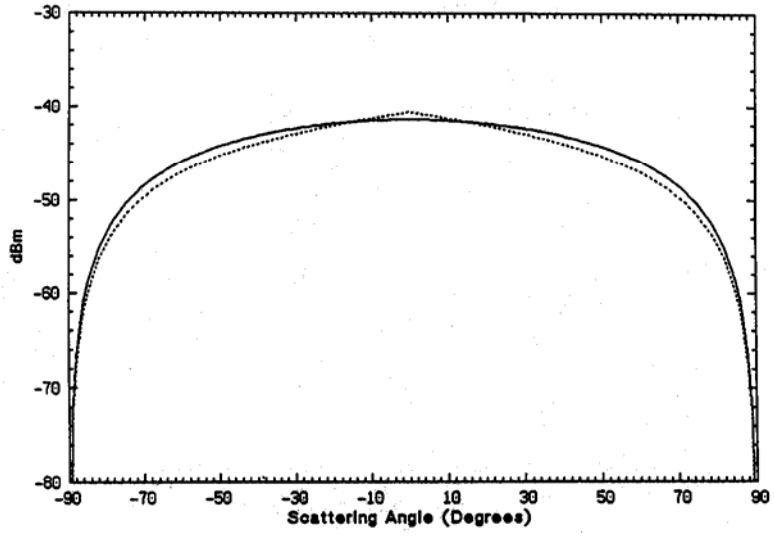

Figure 12. Bistatic echo width of a dielectric hump with $\epsilon = 36 + i17$, $\Delta = 0.3$, and $w = \lambda/15$ over a resistive sheet with $R_0 = 180 + i270$ at $f = 10\,\text{GHz}$ and $\phi_0 = 0$ degrees for H-polarization: (——) numerical technique, (- - - -) perturbation technique.

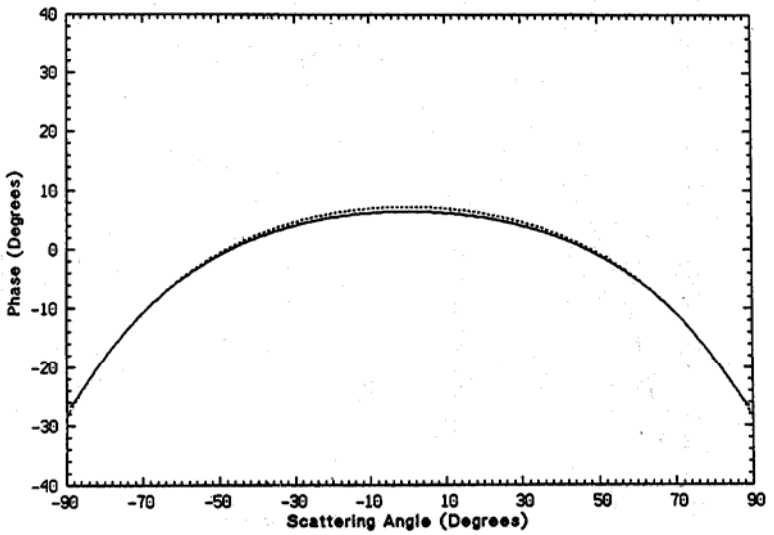

Figure 13. Phase of far field amplitude of a dielectric hump with $\epsilon = 36 + i17, l\ \Delta = 0.3$, and $w = \lambda/15$ over a resistive sheet with $R_0 = 180 + i270$ at $f = 10\,\text{GHz}$ and $\phi_0 = 0$ degrees for H-polarization: (——) numerical technique, (- - - -) perturbation technique.

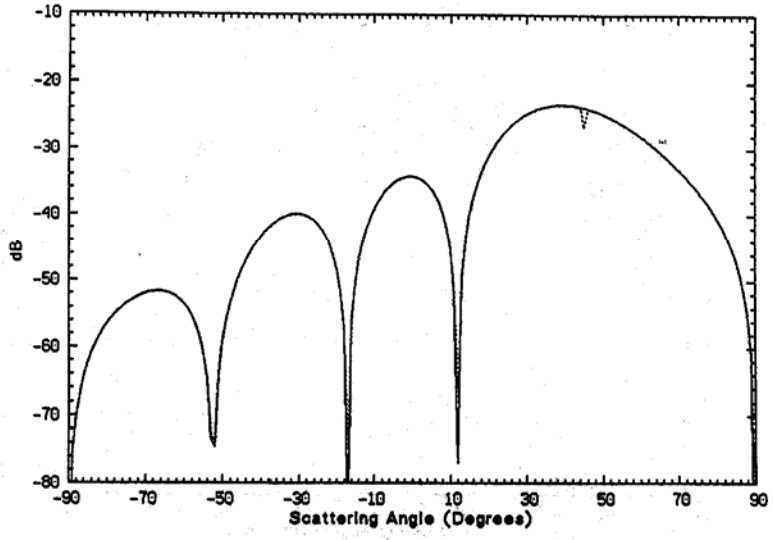

Figure 14. Normalized bistatic echo width (σ/λ) of an impedance insert with $w = 2\lambda$, $\eta_1 = 44 - i44$, $\eta_0 = 40 - i40$ $(\Delta = 0.1)$ at $\phi_0 = 45$ degrees for E-polarization: (——) perturbation technique, (- - - -) GTD technique.

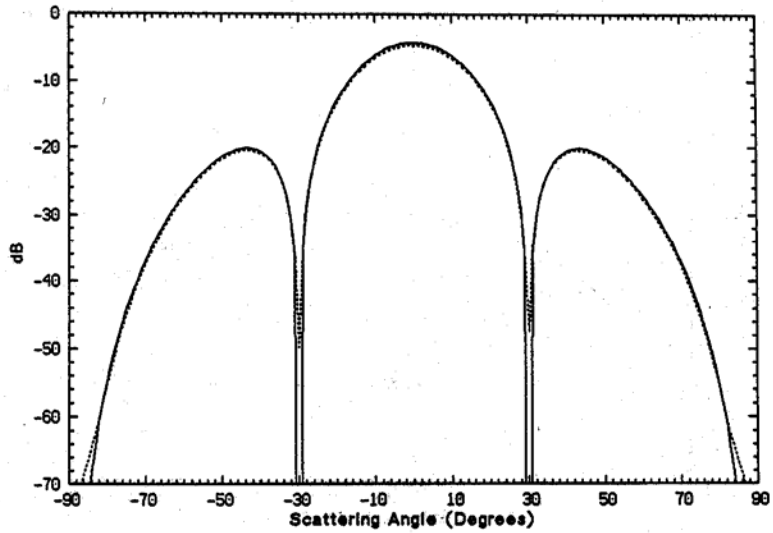

Figure 15. Normalized bistatic echo width (σ/λ) of an impedance insert with $w = 2\lambda$, $\eta_1 = 60 - i60$, $\eta_0 = 40 - i40$ $(\Delta = 0.5)$ at $\phi_0 = 0$ degrees for E-polarization: (——) perturbation technique, (- - - -) GTD technique.

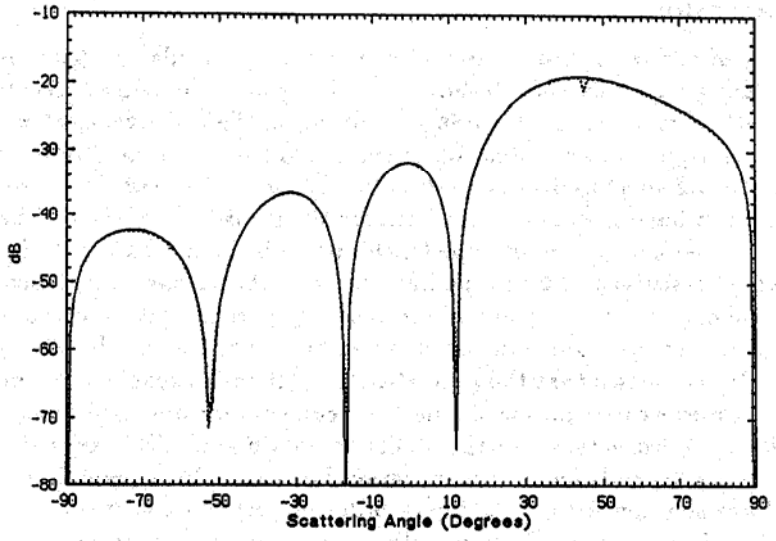

Figure 16. Normalized bistatic echo width (σ/λ) of an impedance insert with $w = 2\lambda$, $\eta_1 = 44 - i44$, $\eta_0 = 40 - i40$ $(\Delta = 0.1)$ at $\phi_0 =$ 45 degrees for H-polarization: (——) perturbation technique, (- - - -) GTD technique.

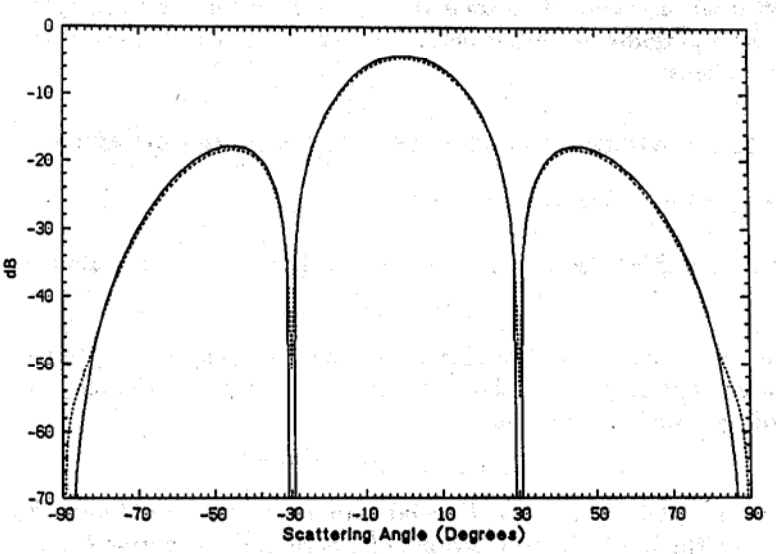

Figure 17. Normalized bistatic echo width (σ/λ) of an impedance insert with $w = 2\lambda$, $\eta_1 = 60 - i60$, $\eta_0 = 40 - i40$ $(\Delta = 0.5)$ at $\phi_0 =$ 0 degrees for H-polarization: (——) perturbation technique, (- - - -) GTD technique.

8. CONCLUSIONS

Problems of scattering from variable resistive and impedance sheets have been studied using a perturbation technique in the Fourier domain. A recursive form for the nth component of the induced current on the resistive sheet was derived that, in principle, allows evaluation of the current to the desired order of perturbation. Having an analytical expression for the induced current in Fourier domain culminates in having an analytical form for the far field amplitude. The solution for the induced current on an impedance surface is identical to that of a resistive sheet whose resistivity is twice the impedance of the surface impedance.

The validity of the technique was checked in two limiting cases where the variation in perturbation function is sharp in either the spatial or the Fourier domain. It was shown that the perturbation method is capable of handling both. The first order expression for the induced current was obtained analytically for an arbitrary perturbation, but the ability to obtain analytical expressions for the higher orders depends on the perturbation function. For a periodic resistivity a closed form solution for any arbitrary order of perturbation was obtained. The results based on the perturbation method were compared with an exact solution based on the moment method as explained in Appendix A. The analytical results were also checked against a GTD solution for the impedance insert problem and the moment method for the problem of a dielectric hump over a resistive sheet as given in [7]. Excellent agreement between the analytical and other methods was observed. It was found that the required order of perturbation is proportional to the perturbation constant Δ and the width of perturbation in spatial domain, i.e., L for a periodic perturbation and w for the impedance insert and dielectric hump problems.

APPENDIX A. NUMERICAL ANALYSIS FOR A PERIODIC RESISTIVE SHEET

A1. Derivation of Green's Function

For a resistive sheet which is periodic in one dimension with period L, we have

$$R(x+L) = R(x) \tag{A1}$$

Suppose the resistive sheet is illuminated by the plane wave given in (5). The induced current on the resistive sheet must satisfy the periodicity requirements imposed by Floquet's theorem, i.e.,

$$J(x+nL) = J(x)e^{ik_0 \sin\phi_0 nL} \tag{A2}$$

The scattered electric field for E-polarization case can be obtained from (6). By subdividing the integral into multiples of a period, the equation can be written as

$$E_y^s = -\frac{k_0 Z_0}{4} \sum_{n=-\infty}^{+\infty} \int_{x_0+nL}^{x_0+(n+1)L} J_y(x') H_0^{(1)}\left(k_0\sqrt{(x-x')^2+z^2}\right) dx' \tag{A3}$$

If the variable x' is now changed to $x'+nL$ and the property (A2) is employed,

8. CONCLUSIONS

Problems of scattering from variable resistive and impedance sheets have been studied using a perturbation technique in the Fourier domain. A recursive form for the nth component of the induced current on the resistive sheet was derived that, in principle, allows evaluation of the current to the desired order of perturbation. Having an analytical expression for the induced current in Fourier domain culminates in having an analytical form for the far field amplitude. The solution for the induced current on an impedance surface is identical to that of a resistive sheet whose resistivity is twice the impedance of the surface impedance.

The validity of the technique was checked in two limiting cases where the variation in perturbation function is sharp in either the spatial or the Fourier domain. It was shown that the perturbation method is capable of handling both. The first order expression for the induced current was obtained analytically for an arbitrary perturbation, but the ability to obtain analytical expressions for the higher orders depends on the perturbation function. For a periodic resistivity a closed form solution for any arbitrary order of perturbation was obtained. The results based on the perturbation method were compared with an exact solution based on the moment method as explained in Appendix A. The analytical results were also checked against a GTD solution for the impedance insert problem and the moment method for the problem of a dielectric hump over a resistive sheet as given in [7]. Excellent agreement between the analytical and other methods was observed. It was found that the required order of perturbation is proportional to the perturbation constant Δ and the width of perturbation in spatial domain, i.e., L for a periodic perturbation and w for the impedance insert and dielectric hump problems.

APPENDIX A. NUMERICAL ANALYSIS FOR A PERIODIC RESISTIVE SHEET

A1. Derivation of Green's Function

For a resistive sheet which is periodic in one dimension with period L, we have

$$R(x+L) = R(x) \tag{A1}$$

Suppose the resistive sheet is illuminated by the plane wave given in (5). The induced current on the resistive sheet must satisfy the periodicity requirements imposed by Floquet's theorem, i.e.,

$$J(x+nL) = J(x)e^{ik_0 \sin\phi_0 nL} \tag{A2}$$

The scattered electric field for E-polarization case can be obtained from (6). By subdividing the integral into multiples of a period, the equation can be written as

$$E_y^s = -\frac{k_0 Z_0}{4} \sum_{n=-\infty}^{+\infty} \int_{x_0+nL}^{x_0+(n+1)L} J_y(x') H_0^{(1)}\left(k_0\sqrt{(x-x')^2+z^2}\right) dx' \tag{A3}$$

If the variable x' is now changed to $x'+nL$ and the property (A2) is employed,

we get

$$E_y^s = -\frac{k_0 Z_0}{4} \int_{x_0}^{x_0+L} J_y(x')\, G_e(x, x', z)\, dx' \tag{A4}$$

where

$$G_e(x, x', z) \equiv \sum_{n=-\infty}^{+\infty} H_0^{(1)} \left(k_0 \sqrt{(x - x' - nL)^2 + z^2} \right) e^{ik_0 \sin\phi_0 nL} \tag{A5}$$

is the Green's function of the problem. The series is very slowly converging, especially when L is small compared to the wavelength. To make the problem computationally tractable a better form for Green's function is needed. If the Fourier integral representation of the Hankel function is inserted into (A5) and the order of summation, integration reversed, we have

$$G_e(x, x', z) = \frac{1}{\pi} \int_{-\infty}^{+\infty} \frac{e^{i\left[\sqrt{k_0^2 - \alpha^2}\,|z| + \alpha(x - x')\right]}}{\sqrt{k_0^2 - \alpha^2}} \sum_{n=-\infty}^{+\infty} e^{-in(\alpha - k_0 \sin\phi_0)L} d\alpha \tag{A6}$$

But

$$\sum_{n=-\infty}^{+\infty} e^{-in(\alpha - k_0 \sin\phi_0)L} = 2\pi \sum_{n=-\infty}^{+\infty} \delta\left[(\alpha - k_0 \sin\phi_0)\, L - 2\pi n\right] \tag{A7}$$

Applying the above identity to (A6) and changing the order of summation and integration one more time provides the following expression for the Green's function:

$$G_e(x, x', z) = \frac{2}{L} \sum_{n=-\infty}^{+\infty} \frac{e^{i\sqrt{k_0^2 - \left(\frac{2\pi n}{L} + k_0 \sin\phi_0\right)^2}\,|z|}}{\sqrt{k_0^2 - \left(\frac{2\pi n}{L} + k_0 \sin\phi_0\right)^2}} e^{i\left(\frac{2\pi n}{L} + k_0 \sin\phi_0\right)(x - x')} \tag{A8}$$

This series converges very fast specially when z is relatively large, and with the aid of this Green's function, the integral equation for the induced current given in (11) becomes

$$R(x)\, J_y(x) = e^{ik_0 \sin\phi_0 x} - \frac{k_0 Z_0}{4} \int_{x_0}^{x_0+L} J_y(x')\, G_e(x, x', 0^+)\, dx' \tag{A9}$$

By a similar technique the Green's function for a periodic resistive sheet in the H-polarization case can be derived and is given by

$$G_h(x, x', z) = \frac{2}{L} \left(1 + \frac{\partial^2}{\partial x^2}\right) \sum_{n=-\infty}^{+\infty} \frac{e^{i\sqrt{k_0^2 - \left(\frac{2\pi n}{L} + k_0 \sin\phi_0\right)^2}\,|z|}}{\sqrt{k_0^2 - \left(\frac{2\pi n}{L} + k_0 \sin\phi_0\right)^2}} \cdot e^{i\left(\frac{2\pi n}{L} + k_0 \sin\phi_0\right)(x - x')} \tag{A10}$$

and the resulting integral equation for the induced current is

$$R(x) J_x(x) = -\cos\phi_0\, e^{ik_0 \sin\phi_0 x} - \frac{k_0 Z_0}{4} \int_{x_0}^{x_0+L} J_x(x')\, G_h(x, x', 0^+)\, dx' \tag{A11}$$

The form of the Green's functions shows that the scattered field is composed of two types of waves: (1) propagating waves and (2) surface waves. The latter decay exponentially away from the surface and there are an infinite number of them. In contrast, the number of propagating waves is finite, depending upon the period L and the angle of incidence. The nth mode is a propagating mode if n belongs to set $\mathcal{N}$ defined by

$$\mathcal{N} = \left\{ n; -\frac{L}{\lambda}(1+\sin\phi_0) < n < \frac{L}{\lambda}(1-\sin\phi_0) \right\} \tag{A12}$$

In the far zone only the propagating modes are observable and the electric field of the nth mode for E-polarization is, for example, given by $(n \in \mathcal{N})$

$$E_y^n = -\left[\frac{k_0 Z_0}{2L} \frac{\int_{x_0}^{x_0+L} J_y(x')\, e^{-i\left(\frac{2\pi n}{L}+k_0\sin\phi_0\right)x'} dx'}{\sqrt{k_0^2 - \left(\frac{2\pi n}{L}+k_0\sin\phi_0\right)^2}} \right] \cdot e^{i\sqrt{k_0^2-\left(\frac{2\pi n}{L}+k_0\sin\phi_0\right)^2}\,|z|}\, e^{i\left(\frac{2\pi n}{L}+k_0\sin\phi_0\right)x} \tag{A13}$$

and for H-polarization we have

$$H_y^n = \mp\left[\frac{1}{2L}\int_{x_0}^{x_0+L} J_x(x')\, e^{-i\left(\frac{2\pi n}{L}+k_0\sin\phi_0\right)x'} dx' \right] \cdot e^{i\sqrt{k_0^2-\left(\frac{2\pi n}{L}+k_0\sin\phi_0\right)^2}\,|z|} e^{i\left(\frac{2\pi n}{L}+k_0\sin\phi_0\right)x} \tag{A14}$$

where the upper and lower signs apply for an observation point in the upper or lower half-spaces respectively. The direction of propagation of each mode is defined by the angle ϕ_n^s measured from the normal to the surface and can be obtained from

$$\sin\phi_n^s = \frac{\lambda}{L}n + \sin\phi_0 \tag{A15}$$

A2. Numerical Analysis

Numerical solutions of the integral equations can be obtained by the method of moments. The unknown current is represented approximately by an expansion of pulse basis functions as

$$J(x) = \sum_{m=1}^{M} J_m P(x - x_m) \tag{A16}$$

where J_m are the unknown coefficients to be found, M is the total number of segments, and $P(x)$ is the pulse function defined by

$$P(x) = \begin{cases} 1, & |x| < \dfrac{\Delta x}{2} \\ 0, & \text{otherwise} \end{cases} \tag{A17}$$

In the case of E-polarization, by substituting $(A16)$ into integral equation $(A9)$ and setting $x_0 = -L/2$ we get

$$R(x)J(x) = e^{ik_0 \sin\phi_0 x} - \frac{k_0 Z_0}{4} \sum_{m=1}^{M} J_m \int_{x_m - \frac{\Delta x}{2}}^{x_m + \frac{\Delta x}{2}} G_e(x, x', 0^+)\, dx' \qquad (A18)$$

After evaluating the integral and setting the observation point at $x = x_k$, the following expression results:

$$R(x_k)J(x_k) = e^{ik_0 \sin\phi_0 x_k} - \frac{k_0 Z_0}{L} \sum_{m=1}^{M} J_m \left[\sum_{n=-\infty}^{+\infty} \frac{e^{i\left(\frac{2\pi n}{L} + k_0 \sin\phi_0\right)(x_k - x_m)} \sin\left(\left(\frac{2\pi n}{L} + k_0 \sin\phi_0\right)\frac{\Delta x}{2}\right)}{\left(\frac{2\pi n}{L} + k_0 \sin\phi_0\right)\sqrt{k_0^2 - \left(\frac{2\pi n}{L} + k_0 \sin\phi_0\right)^2}} \right] \qquad (A19)$$

This can be cast in matrix form as

$$[\mathcal{Z}]\,[\mathcal{J}] = [\mathcal{V}] \qquad (A20)$$

where $[\mathcal{Z}]$ is the impedance matrix and its entries are

$$z_{km} = \frac{k_0 Z_0}{L} \sum_{n=-\infty}^{+\infty} \frac{e^{i\left(\frac{2\pi n}{L} + k_0 \sin\phi_0\right)(x_k - x_m)} \sin\left(\left(\frac{2\pi n}{L} + k_0 \sin\phi_0\right)\frac{\Delta x}{2}\right)}{\left(\frac{2\pi n}{L} + k_0 \sin\phi_0\right)\sqrt{k_0^2 - \left(\frac{2\pi n}{L} + k_0 \sin\phi_0\right)^2}}, \quad k \neq m \qquad (A21)$$

$$z_{kk} = \frac{k_0 Z_0}{L} \sum_{n=-\infty}^{+\infty} \frac{\sin\left(\left(\frac{2\pi n}{L} + k_0 \sin\phi_0\right)\frac{\Delta x}{2}\right)}{\left(\frac{2\pi n}{L} + k_0 \sin\phi_0\right)\sqrt{k_0^2 - \left(\frac{2\pi n}{L} + k_0 \sin\phi_0\right)^2}} + R(x_k), \quad k = m \qquad (A22)$$

$[\mathcal{J}]$ is a column vector whose components are the unknown J_m's and $[\mathcal{V}]$ is the excitation vector whose components are given by

$$v_k = e^{ik_0 \sin\phi_0 x_k} \qquad (A23)$$

Derivation of the impedance matrix for H-polarization is rather difficult because of the higher order singularity of the Green's function. Using the same expansion of the induced current as before and inserting it into the integral equation $(A11)$ we obtain

$$R(x)J(x) = -\cos\phi_0 e^{ik_0 \sin\phi_0 x} - \frac{k_0 Z_0}{4} \sum_{m=1}^{M} J_m \int_{x_m - \frac{\Delta x}{2}}^{x_m + \frac{\Delta x}{2}} \left(1 + \frac{\partial^2}{\partial x^2}\right) G_h(x, x', 0^+)\, dx' \qquad (A24)$$

To find the impedance matrix consider the following integral:

$$\int \frac{\partial^2}{\partial x^2} G_h(x,x',z)\,dx' = -G_h'(x,x',z) \tag{A25}$$

where $G_h'(x,x',z)$ is the derivative of $G_h(x,x',z)$ with respect to x and is given by

$$G_h'(x,x',z) = \frac{2}{L}\sum_{n=-\infty}^{+\infty} \frac{e^{i\sqrt{k_0^2-\left(\frac{2\pi n}{L}+k_0\sin\phi_0\right)^2}\,|z|}}{\sqrt{k_0^2-\left(\frac{2\pi n}{L}+k_0\sin\phi_0\right)^2}} \cdot i\left(\frac{2\pi n}{L}+k_0\sin\phi_0\right) e^{i\left(\frac{2\pi n}{L}+k_0\sin\phi_0\right)(x-x')} \tag{A26}$$

The convergence of the series is very poor when $z \to 0$, but the limit does exist. To achieve a better convergence rate, consider the following geometric series based on the asymptotic behavior of the individual terms in (A26) for large n, positive and negative:

$$\begin{aligned} S_1 &= \frac{2}{L}\sum_{n=1}^{+\infty} e^{-\frac{2\pi n}{L}|z|}\, e^{i\left(\frac{2\pi n}{L}+k_0\sin\phi_0\right)(x-x')} \\ &= \frac{2}{L}\, e^{-ik_0\sin\phi_0(x-x')}\, \frac{e^{-\frac{2\pi}{L}(|z|+i(x'-x))}}{1-e^{-\frac{2\pi}{L}(|z|+i(x'-x))}} \end{aligned} \tag{A27}$$

$$\begin{aligned} S_2 &= \frac{2}{L}\sum_{n=-\infty}^{-1} e^{\frac{2\pi n}{L}|z|}\, e^{i\left(\frac{2\pi n}{L}+k_0\sin\phi_0\right)(x-x')} \\ &= \frac{2}{L}\, e^{-ik_0\sin\phi_0(x-x')}\frac{e^{-\frac{2\pi}{L}(|z|-i(x'-x))}}{1-e^{-\frac{2\pi}{L}(|z|-i(x'-x))}} \end{aligned} \tag{A28}$$

By adding and subtracting the above series from $G_h'(x,x',z)$ and then letting $z \to 0$ it follows that

$$\begin{aligned} G_h'(x,x',0^+) = &\lim_{z\to 0}\left[G_h'(x,x',z) - S_1 - S_2\right] \\ &+ \frac{2}{L}\, e^{ik_0\sin\phi_0(x-x')}\left[\frac{e^{-i\frac{2\pi}{L}(x'-x)}}{1-e^{-i\frac{2\pi}{L}(x'-x)}} - \frac{e^{i\frac{2\pi}{L}(x'-x)}}{1-e^{i\frac{2\pi}{L}(x'-x)}}\right] \end{aligned} \tag{A29}$$

which can be rearranged to give

$$\begin{aligned} G_h'(x,x',0^+) = \frac{2}{L}\, e^{-ik_0\sin\phi_0(x-x')}\Bigg\{ &\sum_{n=1}^{+\infty} \\ &\left[\left(\frac{i\left(\frac{2\pi n}{L}+k_0\sin\phi_0\right)}{\sqrt{k_0^2-\left(\frac{2\pi n}{L}+k_0\sin\phi_0\right)^2}}-1\right) e^{-i\frac{2\pi n}{L}(x'-x)}\right. \end{aligned}$$

$$+\left(\frac{i\left(-\frac{2\pi n}{L}+k_0\sin\phi_0\right)}{\sqrt{k_0^2-\left(-\frac{2\pi n}{L}+k_0\sin\phi_0\right)^2}}+1\right)e^{i\frac{2\pi n}{L}(x'-x)}\Bigg]$$

$$+\left[i\tan\phi_0+\frac{e^{-i\frac{2\pi}{L}(x'-x)}}{1-e^{-i\frac{2\pi}{L}(x'-x)}}-\frac{e^{i\frac{2\pi}{L}(x'-x)}}{1-e^{i\frac{2\pi}{L}(x'-x)}}\right]\Bigg\} \quad (A30)$$

The above series is absolutely convergent and its rate of convergence is relatively fast (like $1/n^2$). By defining the following parameters:

$$A(x,x_m)=\frac{1}{k_0^2}\int_{x_m-\frac{\Delta x}{2}}^{x_m+\frac{\Delta x}{2}}\frac{\partial^2}{\partial x^2}G_h(x,x',0^+)\,dx'=\frac{4i}{Lk_0^2}e^{ik_0\sin\phi_0(x-x_m)}$$

$$\cdot\Bigg\{\sum_{n=1}^{+\infty}\Bigg[\left(\frac{i\left(\frac{2\pi n}{L}+k_0\sin\phi_0\right)}{\sqrt{k_0^2-\left(\frac{2\pi n}{L}+k_0\sin\phi_0\right)^2}}-1\right)$$

$$e^{i\frac{2\pi n}{L}(x-x_m)}\sin\left(\left(\frac{2\pi n}{L}+k_0\sin\phi_0\right)\frac{\Delta x}{2}\right)$$

$$+\left(\frac{i\left(-\frac{2\pi n}{L}+k_0\sin\phi_0\right)}{\sqrt{k_0^2-\left(-\frac{2\pi n}{L}+k_0\sin\phi_0\right)^2}}+1\right)$$

$$e^{-i\frac{2\pi n}{L}(x-x_m)}\sin\left(\left(-\frac{2\pi n}{L}+k_0\sin\phi_0\right)\frac{\Delta x}{2}\right)\Bigg]$$

$$+i\tan\phi_0\sin\left(k_0\sin\phi_0\,\frac{\Delta x}{2}\right)$$

$$+\frac{1}{2}\cot\left(\frac{\pi}{L}\left(x-x_m+\frac{\Delta x}{2}\right)\right)e^{i\left(k_0\sin\phi_0\frac{\Delta x}{2}\right)}$$

$$-\frac{1}{2}\cot\left(\frac{\pi}{L}\left(x-x_m-\frac{\Delta x}{2}\right)\right)e^{-i\left(k_0\sin\phi_0\frac{\Delta x}{2}\right)}\Bigg\} \quad (A31)$$

$$B(x,x_m)=\int_{x_m-\frac{\Delta x}{2}}^{x_m+\frac{\Delta x}{2}}G_h\left(x,x',0^+\right)dx'$$

$$=\frac{4}{L}e^{ik_0\sin\phi_0(x-x_m)}\sum_{n=-\infty}^{+\infty}\frac{e^{i\frac{2\pi n}{L}(x-x_m)}\sin\left(\left(\frac{2\pi n}{L}+k_0\sin\phi_0\right)\frac{\Delta x}{2}\right)}{\left(\frac{2\pi n}{L}+k_0\sin\phi_0\right)\sqrt{k_0^2-\left(\frac{2\pi n}{L}+k_0\sin\phi_0\right)^2}} \quad (A32)$$

and setting the observation point $x = x_k$, $(A24)$ can be written as

$$R(x_k)J(x_k) = -\cos\phi_0\, e^{ik_0 \sin\phi_0 x} - \frac{k_0 Z_0}{4} \sum_{m=1}^{M} J_m \left[A(x_k, x_m) + B(x_k, x_m)\right] \quad (A33)$$

This can be cast as a matrix equation similar to $(A20)$ with the impedance matrix and excitation vector having entries

$$z_{km} = \frac{k_0 Z_0}{4} \left[A(x_k, x_m) + B(x_k, x_m)\right], \qquad k \neq m$$

$$z_{kk} = \frac{k_0 Z_0}{4} \left[A(x_k, x_k) + B(x_k, x_k)\right], \qquad k = m \quad (A34)$$

$$v_k = -\cos\phi_0\, e^{ik_0 \sin\phi_0 x_k} \quad (A35)$$

ACKNOWLEDGMENTS

The author would like to thank Prof. T. B. A. Senior and Prof. F. T. Ulaby for their helpful comments and reviewing of this work.

This work was supported by NASA under contract NAG–5–480.

The Editor thanks C. Eftimiu, and three anonymous Reviewers for reviewing the paper.

REFERENCES

1. Bates, R. H. T., and D. J. N. Wall, "Chandrasekhar transformation improve convergence of computation of scattering from linearly stratified media," *IEEE Trans. Antennas Propagat.*,, Vol. 24, 251–251, 1976.
2. Eftimiu, C., and P. L. Huddleston, "Natural frequencies and modes of finite open circular cylinders," *IEEE Trans. Antennas Propagat.*,, Vol. 31, 910–917, 1983.
3. Harrington, R. F., *Time-Harmonic Electromagnetic Fields,* McGraw-Hill, New York, 317, 1961.
4. Herman, M. I., and J. L. Volakis, "High frequency scattering from polygonal impedance cylinders and strips," *IEEE Trans. Antennas Propagat.,* Vol. 36, 679–688, 1988.
5. Maliuzhinets, G. D., "Excitation, reflection and emission of surface waves from a wedge with given face impedances," *Sov. Phys. Dokl.,* Engl. Transl., Vol. 3, 752–755, 1958.
6. Rice, S. O., "Reflection of electromagnetic waves from slightly rough surfaces," *Commun. Pure Appl. Math.,* Vol. 4, 361–378, 1951.
7. Sarabandi, K., "Scattering from variable resistive and impedance sheets," *Radiation Laboratory Report No. RL–863,* The University of Michigan, March 1989.
8. Senior, T. B. A., "Scattering by resistive strips," *Radio Science,* Vol. 14, 911–924, 1979.
9. Senior, T. B. A., K. Sarabandi, and F. T. Ulaby, "Measuring and modeling the backscattering cross section of a leaf," *Radio Science,* Vol. 22, 1109–1116, 1987.
10. Senior, T. B. A., and J. L. Volakis, "Sheet simulation of a thin dielectric layer," *Radio Science,* Vol. 22, 1261–1272, 1987.
11. Stephen, L. R., P. Diament, and S. P. Schlesinger, "Perturbation analysis of axially nonuniform electromagnetic structures using nonlinear phase progression," *IEEE Trans. Antennas Propagat.,* Vol. 15, 422–430, 1967.

Kamal Sarabandi was born in Tehran, Iran on November 4, 1956. He received the B.S. degree in electrical engineering from Sharif University of Technology, Tehran, Iran, in 1980. From 1980 to 1984 he worked as a microwave engineer in Iran's Telecommunication Research Center. In Fall 1984 he joined the graduate program at the University of Michigan. There he received M.S.E. and Ph.D. degrees in electrical engineering in 1986 and 1989 respectively. He also received the M.S. degree in mathematics in 1989 from the University of Michigan. Currently he is with the Department of Electrical Engineering and Computer Science at the University of Michigan. His research interests include electromagnetic scattering and microwave remote sensing.